Physica A 466 (2017) 10–20

Contents lists available at ScienceDirect

Physica A

journal homepage: www.elsevier.com/locate/physa

Assembly of magnetic spheres in strong homogeneous magnetic field

René Messina [a,*], Igor Stanković [b]

[a] Equipe BioPhysStat, LCP-A2MC, IJB FR CNRS 2843, Université de Lorraine, 1 Boulevard Arago, 57070 Metz, France

[b] Scientific Computing Laboratory, Institute of Physics Belgrade, University of Belgrade, Pregrevica 118, 11080 Belgrade, Serbia

HIGHLIGHTS

- Phase diagram of ground states for finite number of magnetic beads in strong external field.
- Two-chain state characterized by tails of constant size.
- Relevance of the key interaction between a chain and a single bead.

ARTICLE INFO

Article history:
Received 7 March 2016
Received in revised form 26 August 2016
Available online 9 September 2016

Keywords:
Dipolar interaction
Self-assembly
Magnetic chains
Soft matter
Granular media

ABSTRACT

The assembly in two dimensions of spherical magnets in strong magnetic field is addressed theoretically. It is shown that the attraction and assembly of parallel magnetic chains is the result of a delicate interplay of dipole–dipole interactions and short ranged excluded volume correlations. Minimal energy structures are obtained by numerical optimization procedure as well as analytical considerations. For a small number of constitutive magnets $N_{\text{tot}} \leq 26$, a straight chain is found to be the ground state. In the regime of larger $N_{\text{tot}} \geq 27$, the magnets form two touching chains with equally long tails at both ends. We succeed to identify the transition from two to three touching chains at $N_{\text{tot}} = 129$. Overall, this study sheds light on the mechanisms of the recently experimentally observed ribbon formation of superparamagnetic colloids via lateral aggregation of magnetic chains in magnetic field (Darras et al., 2016).

1. Introduction

There are several reasons for strong and growing interest in self-assembled structures of dipolar particles (i.e., with electric or magnetic dipoles). On the technological side, such systems have enormous potential applications. For instance, manufacturing of novel optical and stimuli-responsive materials is based on self assembly of magnetic particles [1,2]. On the other hand, dipolar particles and the resulting phases can be well tuned by imposing an external field [3,4]. Assemblies of magnetic particles are known to produce a plethora of one-, two-, and three dimensional objects (e.g., chains, rings, and even tubes) [5–7]. Experimental evidence of spontaneous assembly of small magnetic nanocubes into highly ordered chains, sheets, and cuboids in solution by applying a magnetic field was recently reported [8]. Equally intriguing microstructures such as Saturn ring- or flower-like structures were also found experimentally for a mixture of paramagnetic and diamagnetic colloidal particles within a magnetized ferrofluid [9]. From the perspective of biophysics, magnetic particles can be regarded

* Corresponding author.
E-mail addresses: rene.messina@univ-lorraine.fr (R. Messina), igor.stankovic@ipb.ac.rs (I. Stanković).

http://dx.doi.org/10.1016/j.physa.2016.08.079
0378-4371/

as a model system for probing the polar organization of microtubules [10] or generating spontaneous helical superstructures [11,12] reminiscent of DNA molecules.

By essence, the dipole–dipole driving force for self-assembly is long range and highly anisotropic (i.e., non-central pair potential) [13,14] and therefore represents a formidable theoretical challenge. In this spirit, the pioneering theoretical work of Jacobs and Beans [15] and later that of de Gennes and Pincus [16] about the microstructure of self-assembled (spherical) magnets shed some light on the ordering mechanisms. More recently, microstructures of dipolar fluids have been thoroughly studied by computer simulations [17–19] and in experiments [20]. There, an important common feature is the formation of chains [17,19] and possibly in presence of an external magnetic field [18,20]. The interaction of two *infinite* chains in strong external magnetic field was studied analytically in the early 90's [21,22]. Depending on their relative shift, short-range attractions/repulsion sets in with a roughly exponential decay. With all that being said, only recently, the ground state structures of magnetic spheres without external magnetic field have been properly addressed in three dimensions [6,23,24] as well as in two dimensions [7].

The goal of the present contribution is to tackle the fascinating problem of self-assembly of magnets under strong magnetic field in a physically simple and transparent framework. Motivated by the self-assembly experimentally revealed with a small number of magnetic beads [8,9,25,26], we explore (effective) interactions and assemblies of a finite number of magnetic beads with *parallel dipoles* (e.g., as obtained by a strong external magnetic field) and confined in two dimensions (e.g., by gravity [26] and/or by capillarity at liquid/liquid interface [25]).[1] When dealing with the search of the ground state, we utilize two fully different routes to calculate the energy minimum of the system: (i) genetic algorithm and (ii) direct calculation and comparison of the energy of different configurations. The paper is organized as follows: In Section 2 we expose the magnetic chains Hamiltonian. Section 3 is devoted to the analytical results dealing with the two-chain state. Phase diagram of self-assembled magnets obtained by numerical genetic algorithm is discussed in Section 4. Concluding remarks are provided in Section 5.

2. Model

2.1. Pair interaction potential

We begin by considering two magnetic hard spheres of diameter d separated by a distance $r_{12} = |\vec{r}_2 - \vec{r}_1| > d$, where $\vec{r}_1$ and $\vec{r}_2$ represent the position vectors of the centers of particle 1 and particle 2, respectively. These spherical magnets being also characterized by a magnetic moment $(\vec{m}_1, \vec{m}_2)$, the pair potential energy is dictated by:

$$U(\vec{r}_{12}) = C\frac{1}{r_{12}^3}\left[\vec{m}_1\cdot\vec{m}_2 - 3\frac{(\vec{m}_1\cdot\vec{r}_{12})(\vec{m}_2\cdot\vec{r}_{12})}{r_{12}^2}\right], \tag{1}$$

where C is a constant that depends on the intervening medium (e.g., for vacuum $C = \frac{\mu_0}{4\pi}$ with μ_0 being the vacuum permeability).

The approach we adopt in this work is based on the calculation of the magnetic energy of various configurations of spheres in externally imposed magnetic field $\vec{B} = B\vec{e}_x$ aligned with x-axis. We assume that the external magnetic field is strong, i.e, $B \gg mC\frac{1}{d^3}$ (with $m := |\vec{m}_1| = |\vec{m}_2|$), so that all dipole moments in the system are aligned with $\vec{B}$ and hence parallel to the x-axis, i.e. $\vec{m} = m\vec{e}_x$. In this limit of strong field, the pair potential (1) becomes

$$U(\vec{r}_{12}) = C\frac{m^2}{r_{12}^3}\left[1 - 3\frac{(x_2 - x_1)^2}{r_{12}^2}\right]. \tag{2}$$

2.2. Chains Hamiltonian

It is convenient to introduce the energy scale defined by $U_{\uparrow\uparrow} \equiv \frac{Cm^2}{d^3}$ that physically represents the repulsive potential value for two parallel dipoles at contact standing side by side as clearly suggested by the notation. The dipoles attract if placed with head-to-tail (i.e., $\rightarrow\rightarrow$). The latter promotes formation of one dimensional chains consisting of many dipoles (i.e., $\rightarrow\rightarrow\ldots\rightarrow$). The reduced total potential energy of interaction of a system consisting of two chains made up of N_1 and N_2 particles, $U^{tot}_{N_1N_2}$, can be written as

$$U^{\text{tot}}_{N_1N_2} = \frac{1}{2}\sum_{\substack{i,j=1\\ i\neq j}}^{N_1+N_2}\frac{U(\vec{r}_{ij})}{U_{\uparrow\uparrow}} \quad (r_{ij}\geq d). \tag{3}$$

[1] Note that our model corresponds to a zero temperature approach where fluctuations (for instance in chain length and/or shape) [27] are neglected. Hence, when comparing theory vs experiments, one has to bear in mind that only the high magnetic coupling (external field) is relevant. This limit is typically reached in magnetorheological fluids or superparamagnetic colloids with saturated magnetization under the influence of a strong external field.

The sum in Eq. (3) can be separated into three terms,

$$U^{tot}_{N_1N_2} = U^{1c}_{N_1} + U^{1c}_{N_2} + U^{cc}_{N_1N_2}, \tag{4}$$

where $U^{1c}_{N_{1,2}}$ are the reduced *intra-chain* contributions to the total energy, whereas $U^{cc}_{N_1N_2}$ is the *inter-chain* (or cross chain) contribution to the total energy.

More explicitly, the reduced intra-chain energy U^{1c}_N is given by

$$U^{1c}_N = \sum_{i=1}^{N-1}\sum_{j=i+1}^{N} \frac{U(\vec{r}_{ij})}{U_{\uparrow\uparrow}} \quad (r_{ij} \geq d) \tag{5}$$

respecting the non-overlapping conditions. Thereby, the expression for U^{1c}_N in reduced units is merely given by

$$U^{1c}_N = -\sum_{i=1}^{N-1}\sum_{j=i+1}^{N} \frac{2}{(j-i)^3} = -2\sum_{i=1}^{N-1} \frac{N-i}{i^3}. \tag{6}$$

This always negative energy in Eq. (6) can be seen as the *cohesive* energy of a magnetic chain. On the other hand, the inter-chain term $U^{cc}_{N_1N_2}$ in Eq. (4) can be either positive or negative depending on the relative x-shift of the two chains. Assume chain 1 has its first bead at $x^{(1)}_1$ so that its last one is at $x^{(N_1)}_1 = x^{(1)}_1 + N_1 d$. Given the symmetry of the system, chain 2 position is then fully specified by the position of its first bead $x^{(1)}_2 = x^{(1)}_1 + \delta_x d$, with δ_x representing the relative x-shift of the two chains. The relative position of two beads i and j belonging to chain 1 and chain 2, respectively, can be written as $\vec{r}_{ij}/d = (j-i+\delta_x, \delta_y)$, where δ_y is the relative (reduced) y-position of the two chains. We then arrive at the simple expression for cross chain interaction energy

$$U^{cc}_{N_1N_2}(\delta_x, \delta_y) = \sum_{i=1}^{N_2}\sum_{j=1}^{N_1} \left\{ \frac{1}{[(j-i+\delta_x)^2 + \delta_y^2]^{\frac{3}{2}}} - \frac{3(j-i+\delta_x)^2}{[(j-i+\delta_x)^2 + \delta_y^2]^{\frac{5}{2}}} \right\}. \tag{7}$$

The effective force between these two chains in the direction perpendicular to the external magnetic field is then given by $F^{cc}_y = -\nabla_{\delta_y} U^{cc}_{N_1N_2}(\delta_x, \delta_y)$. Hence, when talking about attraction vs repulsion, it is the sign of that effective force F^{cc}_y (or $F^{cc}_x = -\nabla_{\delta_x} U^{cc}_{N_1N_2}$ for the component in the field direction) that will matter.

3. Interaction of two chains

3.1. Chain–dipole interaction

It is instructive to first consider the interaction between a chain and a single magnet. Thereby, the most elementary situation consists of a single magnet (i.e., $N_1 = 1$) interacting with a dimer (i.e., $N_2 = 2$). An important configuration is that corresponding to a triangle, see inset in Fig. 1 for $N = 2$, since this is also the local configuration of an infinite triangular lattice. Thereby, the (equilateral) triangle configuration energy is merely given by $U^{cc}_{12}(\delta_x = 1/2, \delta_y = \sqrt{3}/2) = 1/2$, see also Fig. 1. The positive value indicates that there is a strong energy penalty upon assembling a magnetic dimer and a single magnet together into a triangle from infinite relative separation. This feature is fully consistent with the geometrical idea that 60° is larger than the magic angle (54.7°) [13]. Interestingly, upon slightly separating the two objects (keeping $\delta_x = 1/2$), there is a slight increase in energy proving an effective attraction, see Fig. 1. At large separation, one recovers the behavior of two point-like dipoles leading to a typical repulsion scaling as $1/\delta_y^3$. It is to say that there is (always) an *energy barrier* upon assembling a dimer with a distant monomer into a triangular cluster.

When increasing the chain size by the same amount on both ends, the energy at contact for a flat T-shaped configuration is significantly decreased, see Fig. 1. This is merely due to the attractive terms stemming from the interaction between the further dipoles of the chain with the single aside magnet. This energy at contact becomes asymptotically $U^{cc}_{1\infty}(\delta_y = \sqrt{3}/2) \simeq -0.356$ for an infinite chain. Concomitantly, the energy barrier upon approaching a magnet from infinity virtually vanishes when the chain gets very large, see Fig. 1. More specifically, the barrier height strongly diminishes with chain size N_c. Concomitantly, the maximum position in the energy profile is shifted to larger δ_y upon increasing N_c.

Thus, chain size qualitatively matters, and peripheral dipoles along the chain screen the repulsion between the aside magnet and its first neighbors. At small δ_y-separation, deep minima are attained (see Fig. 1) showing that the interaction strength with satellite dipoles overcompensates that with first neighbors.[2]

[2] Note that the behavior of U_{1N} as a function of longitudinal shift δ_x is much more complicated (strong local oscillations can set in for sufficiently close δ_x-overlapping objects) and is not further discussed here. Nonetheless, for symmetry reasons, the lowest energy always occurs at $\delta_x = N/2$ if $\delta_y \geq \sqrt{3}/2$.

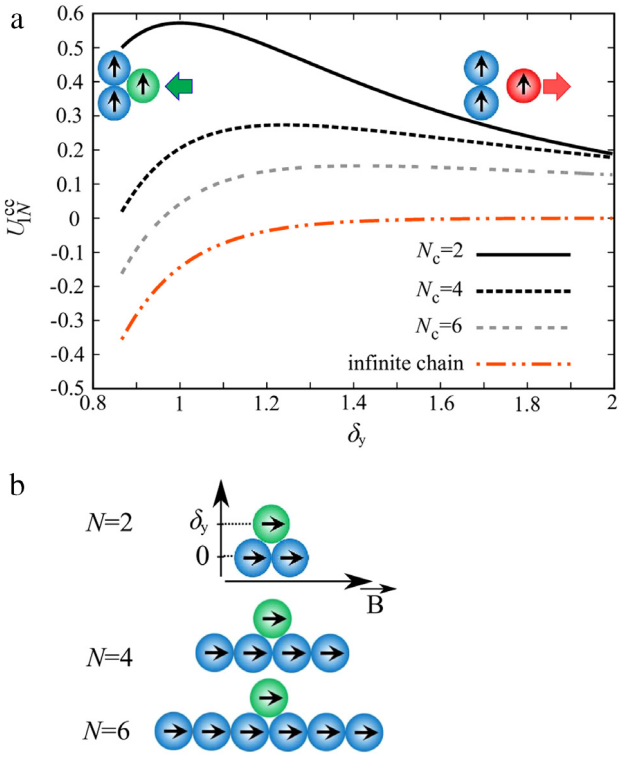

Fig. 1. (a) Reduced cross energy profile of a single magnet interacting with a chain made up of N_c magnetic beads. The center of the single magnet is located at a δ_y distance from the chain and always at the x-mid-position of the latter. (b) Sketch at contact for $N_c = 2, 4, 6$ where $\delta_y = \sqrt{3}/2$.

3.2. Two-chain state

3.2.1. Like sized chains

We now would like to provide a more quantitative analysis of interaction of two equally long chains. Taking advantage of the symmetry the cross energy expression with respect to indices when $N_1 = N_2 = N$ in Eq. (7), we find:

$$U_{NN}^{CC}(\delta_x, \delta_y) = \sum_{i=-N+1}^{N-1} (N - |i|) \left\{ \frac{1}{[(i+\delta_x)^2 + \delta_y^2]^{\frac{3}{2}}} - \frac{3(i+\delta_x)^2}{[(i+\delta_x)^2 + \delta_y^2]^{\frac{5}{2}}} \right\}. \tag{8}$$

The profiles of the interaction potential of two chains with $N = 20$ particles can be found in Fig. 2. In this scenario, we want to illustrate the crucial effect of *positional lateral correlations*. As expected, the strongest repulsion occurs for chains standing exactly face to face with zero lateral shift (i.e., $\delta_x = 0$), see Fig. 2. A small shift amount, here $\delta_x = 1/2$ (see Fig. 2), drastically changes the situation where now effective attraction takes place at short transverse δ_y-separation. Differently said, self-assembly with $\delta_x = 1/2$ is now favored where the lowest energy is obtained at contact with local high packing,[3] see Fig. 2. Upon increasing the relative lateral shift δ_x between the chains, a similar behavior is observed. More specifically, shifted chains with beads standing exactly face to face (i.e., for δ_x assuming integer values, say n) always lead to higher energy δ_y-profiles than with $\delta_x = n + 1/2$, especially near contact, see Fig. 2(b). Besides, the near field repulsion observed for integer values of δ_x switches to attraction if particles of one chain are in the x-middle-point positions of the other chain ones (i.e., for $\delta_x = 0.5$, 5.5, and 12.5), see Fig. 2.[4]

In the far field limit (i.e., $\delta_y/N \gg 1$), magnetic chains should behave as super dipoles, i.e., point-like dipoles with strength Nm. Indeed, at sufficiently large chain–chain distance, repulsion sets in with a $1/\delta_y^3$ power law dependence on distance, see inset in Fig. 2(a). The point where near field attraction switches into repulsion can be understood as crossover between far and near field behavior. As a matter of fact, lateral correlations between discrete finite magnets are essential to promote effective attraction between (weakly shifted) facing chains within distances that are of the order of the bead size.

[3] We have carefully checked that the deepest minimum for $0 < \delta_x < 1$ occurs at contact and for $\delta_x = 0.5$ as intuitively expected. A possible way to kinetically overcome the potential barriers stemming from those oscillations is to temporarily reverse (or counteract) the magnetic field exerted on one chain.

[4] A possible way to kinetically overcome the potential barriers stemming from those potential oscillations is to temporarily reverse (or counteract) the magnetic field exerted on one chain.

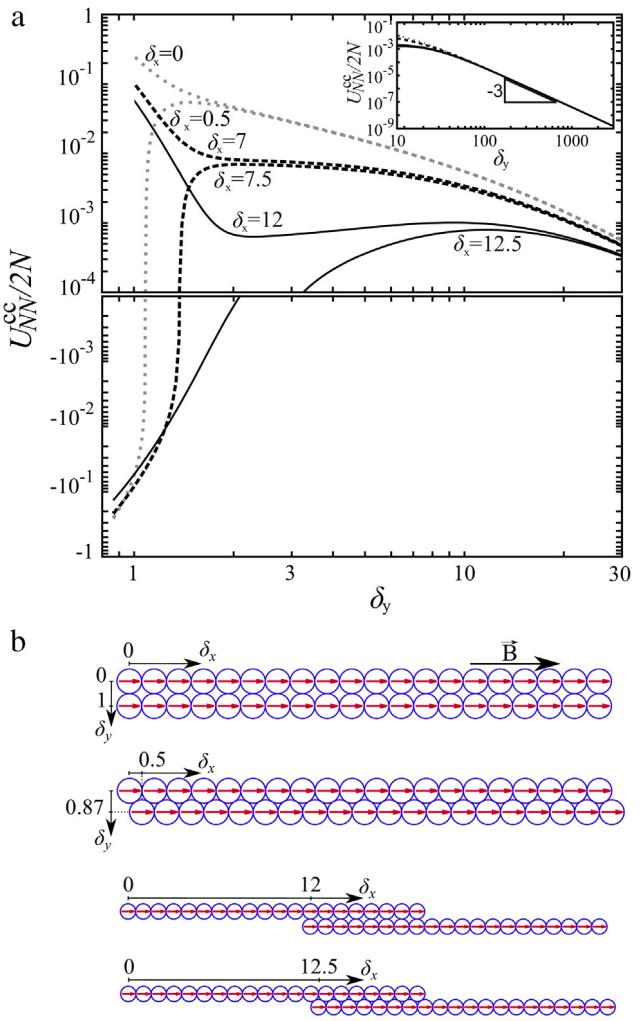

Fig. 2. (a) Interchain interaction energy (per particle) profile as a function of the reduced transverse chain–chain δ_y-separation for different values of the lateral chain–chain reduced shift δ_x. Notice the breaking in the energy-axis allowing logarithmic scale for positive and negative values. The inset shows a wider range of δ_y. (b) Microstructures of chains at contact for different values of δ_x oriented in the magnetic field $\vec{B}$ direction.

To isolate the effects of lateral displacement along the chain axis (or equivalently the external magnetic field), we consider two touching equally long chains exhibiting locally a densely packed triangular structure, see microstructures in Fig. 3. It is useful in this context to introduce integer values of displaced beads via the relation $\delta_x = \delta + 1/2$. Here the value of δ tells about the tail length, i.e., the number of beads of one chain end that are not in contact with the other chain, see Fig. 3 for illustrative configurations with $\delta = 0, 2, 5, 9$. The total energy of our two assembled chains, $U^{ass}_{2N} \equiv U^{tot}_{NN}(\delta + 1/2, \sqrt{3}/2)$, can be written according to Eq. (4) as a sum of (i) twice the single chain cohesive energy $2U^{1c}$ and (ii) the cross chain energy U^{cc}:

$$U^{ass}_{2N}(\delta) = 2U^{1c}_{N} + U^{cc}_{NN}(\delta + 1/2, \sqrt{3}/2). \tag{9}$$

In a similar way that Eq. (6) has been derived, regrouping of repeating terms in the double sum [see Eq. (7)] involved in $U^{cc}_{NN}(\delta + 1/2, \sqrt{3}/2)$ entering Eq. (9) leads to a simple single sum expression given by

$$U^{cc}_{NN}(\delta + 1/2, \sqrt{3}/2) = \sum_{i=-N+1}^{N-1} (N - |i|) \left\{ \frac{1}{\left[\left(i + \delta + \frac{1}{2}\right)^2 + \frac{3}{4}\right]^{\frac{3}{2}}} - \frac{3\left(i + \delta + \frac{1}{2}\right)^2}{\left[\left(i + \delta + \frac{1}{2}\right)^2 + \frac{3}{4}\right]^{\frac{5}{2}}} \right\}. \tag{10}$$

Profiles of the total energy per particle, $U^{ass}_{NN}(\delta)/2N$, as a function of the relative lateral displacement δ are displayed in Fig. 3 for three chain lengths ($N = 6, 10, 26$). For short chains (here $N = 6$) two minima are setting in, see Fig. 3. The first and *lowest* minimum occurs at $\delta = 2$. Its origin is a subtle balance between (i) a positive contribution due to first neighbor

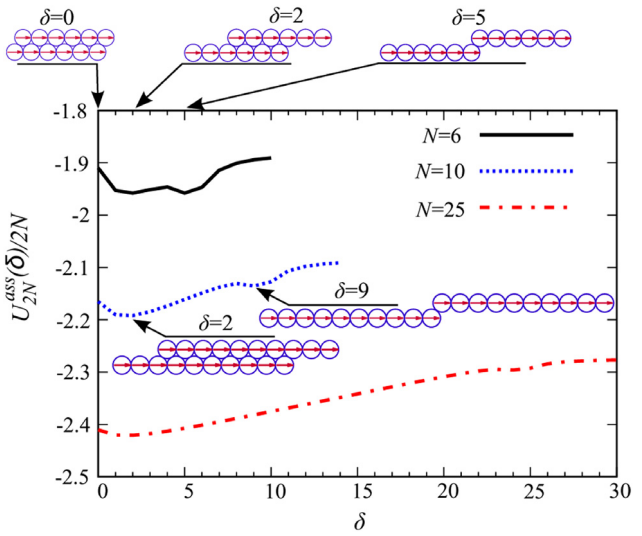

Fig. 3. Total reduced energy per particle, $U_{NN}^{ass}(\delta)/2N$, as a function of the relative lateral displacement δ. Microstructures corresponding to minima are shown for $N = 6, 10$. Note that only the range $\delta \leq N - 1$ corresponds to touching chains as clearly illustrated by the depicted microstructures.

interactions and (ii) a negative contribution due to distant neighbor interactions. These two mechanisms were clearly identified in Section 3.1, see also Fig. 1. Since at $\delta = 5$ the chains do not overlap (only touching ends), the second observed minimum is purely a result of distant neighbor interactions, see Fig. 3. As the chain length is increased ($N = 10, 26$) these features persist: (i) always a lowest minimum at $\delta = 2$ and (ii) a second minimum at chain–chain separation (i.e., $\delta = N-1$), see Fig. 3.

At this point, we would like to answer the following intriguing question: Does the particular $\delta = 2$ shift value always correspond to the ground state for two like sized chains? In other words, when two identical magnetic chains self-assemble in their ground state, do they always exhibit three-bead long tails at both ends? To rationalize this striking finding, we consider the following observable

$$\Delta U_{2N}^{ass}(\delta) = U_{2N}^{ass}(\delta) - U_{2N}^{ass}(\delta - 1) \tag{11}$$

which is merely the energy difference of two states at δ and $\delta - 1$, respectively.[5] Since the cohesive energy is unchanged at prescribed chain size N, the discrete energy variation $\Delta U_{2N}^{ass}(\delta)$ given by Eq. (11) reads

$$\Delta U_{2N}^{ass}(\delta) = \sum_{i=N-\delta}^{N+\delta+1} \left\{ \frac{1}{\left[\left(i-\frac{1}{2}\right)^2 + \frac{3}{4}\right]^{\frac{3}{2}}} - \frac{3(i-\frac{1}{2})^2}{\left[\left(i-\frac{1}{2}\right)^2 + \frac{3}{4}\right]^{\frac{5}{2}}} \right\} - \sum_{i=-\delta}^{\delta+1} \left\{ \frac{1}{\left[\left(i-\frac{1}{2}\right)^2 + \frac{3}{4}\right]^{\frac{3}{2}}} - \frac{3\left(i-\frac{1}{2}\right)^2}{\left[\left(i-\frac{1}{2}\right)^2 + \frac{3}{4}\right]^{\frac{5}{2}}} \right\}. \tag{12}$$

Profiles of $\Delta U_{2N}^{ass}(\delta)$ are shown in Fig. 4 for finite N. It clearly illustrates the behavior of $\Delta U_{2N}^{ass}(\delta)$ with respect to δ and N. More specifically, for overlapping chains (i.e., $\delta \leq N - 1$), the energy variation $\Delta U_{2N}^{ass}(\delta)$ increases at given δ with growing chain size N, see Fig. 4. Moreover, $\Delta U_{2N}^{ass}(\delta)$ assume positive values for $2 < \delta < N - 1$.[6] For large N, the second term in Eq. (12) converges to zero, so that the behavior of $\Delta U_{2N}^{ass}(\delta)$ is solely dictated by the first term. A straightforward summation leads to $\lim_{N\to\infty} \Delta U_{2N}^{ass}(\delta = 2) \simeq -0.019 < 0$ and $\lim_{N\to\infty} \Delta U_{2N}^{ass}(\delta = 3) \simeq +0.162 < 0$. This demonstrates that $\delta = 2$ is indeed the ground state of two assembled like sized chains.

3.2.2. Unlike sized chains

In case of uneven total number of particles $(2N + 1)$, we pay attention to the important situation of two symmetrically placed chains with $N + \delta + 1$ and $N - \delta$ beads, see Fig. 5 for an illustration with $\delta = 2$.[7] The energy of this system denoted by $U_{2N+1}^{ass}(\delta)$ is given by

$$U_{2N+1}^{ass}(\delta) = U_{N-\delta}^{1c} + U_{N+\delta+1}^{1c} + U_{N-\delta,N+\delta+1}^{cc}(\delta + 1/2, \sqrt{3}/2),$$

[5] $\Delta U_{NN}^{ass}(\delta)$ can also be seen as the backward discrete derivative of U_{NN}^{ass} with respect to δ.

[6] Note that the (positive) maximum in $\Delta U_{2N}^{ass}(\delta)$ occurs about half-chain shifts $\delta = N/2$.

[7] Using a genetic algorithm in the next section it will be confirmed that ground state configurations (i.e., with minimal energy) belong indeed to this family of structures.

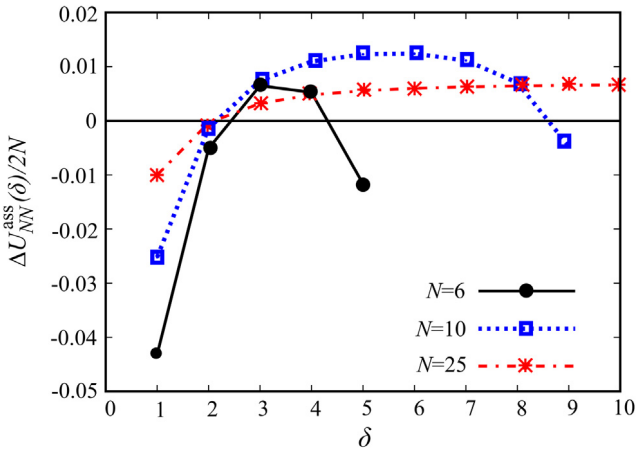

Fig. 4. Profiles of the discrete energy variation $\Delta U_{NN}^{\text{ass}}(\delta)$ as a function of the relative lateral displacement δ for finite different values of N. Only the range $\delta \leq 10$ with interchain touching beads is shown for clarity.

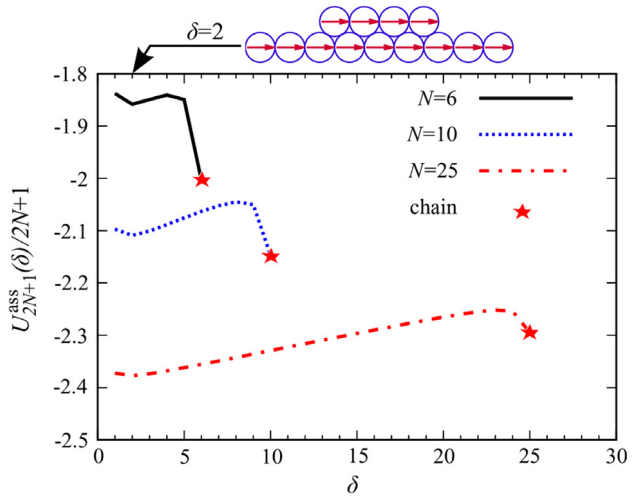

Fig. 5. Total reduced energy per particle, $U_{2N+1}^{\text{ass}}(\delta)/(2N+1)$, as a function of the relative lateral displacement δ. The microstructure corresponding to the ground state (in the imposed two-chain regime) with $N = 6$ for $\delta = 2$ is shown at the top. The special case of $\delta = N$ corresponding to a *single chain* made up of $2N + 1$ beads is denoted by a star.

where the cross chain term reads

$$U_{N-\delta,N+\delta+1}^{\text{cc}}(\delta + 1/2, \sqrt{3}/2) = 2\sum_{i=0}^{N-1} \min(N - i, N - \delta) \times \left\{ \frac{1}{\left[\left(i+\frac{1}{2}\right)^2 + \frac{3}{4}\right]^{\frac{3}{2}}} - \frac{3\left(i+\frac{1}{2}\right)^2}{\left[\left(i+\frac{1}{2}\right)^2 + \frac{3}{4}\right]^{\frac{5}{2}}} \right\}, \tag{13}$$

and the intra-chain terms $U_{N-\delta}^{\text{1c}}$ and $U_{N+\delta+1}^{\text{1c}}$ are specified by Eq. (6). Typical relevant profiles of $\Delta U_{2N+1}^{\text{ass}}(\delta)$ as given by Eq. (13) are shown in Fig. 4 for finite N. Again, the value $\delta = 2$ plays a special role in the energy minimum of assembled chains, see Fig. 5. It can be emphasized that, in the regime of touching chains (i.e., when $\delta \leq N - 1$), a *single* minimum appears and always at $\delta = 2$, see Fig. 5. It is interesting to notice that for a given number of total particles $2N + 1$, the two-chain structure beats energetically the single-chain one only when N is large enough, see Fig. 5.[8]

[8] A similar conclusion could be drawn for like sized chains, see Fig. 3.

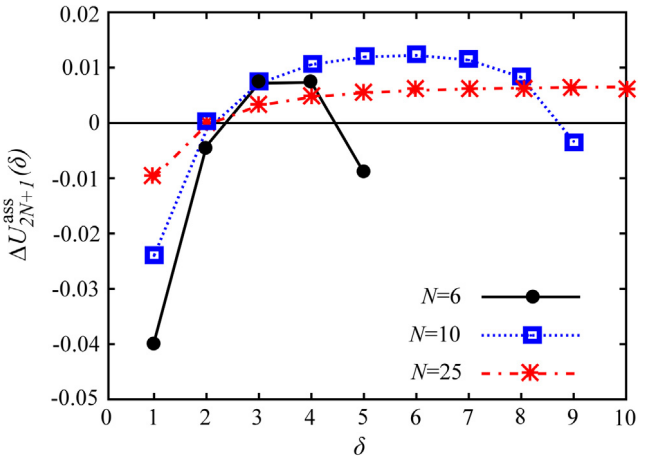

Fig. 6. Profiles of the discrete energy variation $\Delta U^{ass}_{2N+1}(\delta)$ as a function of the relative lateral displacement δ for different values of N. Only the range $\delta \leq 10$ with interchain touching beads is shown for clarity.

In the same spirit of Eq. (11), we define the discrete energy change $\Delta U^{ass}_{2N+1}(\delta)$ upon variation of lateral displacement δ as $\Delta U^{ass}_{2N+1}(\delta) = U^{ass}_{2N+1}(\delta) - U^{ass}_{2N+1}(\delta - 1)$. It is a simple matter to show that this quantity reads

$$\Delta U^{ass}_{2N+1}(\delta) = -2 \sum_{i=N-\delta+1}^{N+\delta} \frac{1}{i^3} - 2 \sum_{i=0}^{\delta-1} \left\{ \frac{1}{\left[\left(i+\frac{1}{2}\right)^2 + \frac{3}{4}\right]^{\frac{3}{2}}} - \frac{3\left(i+\frac{1}{2}\right)^2}{\left[\left(i+\frac{1}{2}\right)^2 + \frac{3}{4}\right]^{\frac{5}{2}}} \right\}, \tag{14}$$

where the first sum in Eq. (14) stems from intrachain interactions, and the second one from cross chain interactions. The behavior of $\Delta U^{ass}_{2N+1}(\delta)$ is sketched in Fig. 6. We observe that the energy difference changes sign from negative to positive around $\delta = 2$, which indicates a minimum in energy there, see Fig. 6. This minimum will also persist at large N. Indeed, we learn from Eq. (14) that for large N only the interchain correlations will survive. In details, a straightforward summation leads to $\lim_{N\to\infty} \Delta U^{ass}_{2N+1}(\delta = 2) \simeq -0.0188 < 0$ and $\lim_{N\to\infty} \Delta U^{ass}_{2N+1}(\delta = 3) \simeq 0.1623 > 0$. Therefore, we can conclude that two symmetrically placed touching chains of length $N + 3$ and $N - 2$ represent an energy minimum for any N larger than two.

3.2.3. Summary

Two chains self-assemble in a minimal energy configuration by building short *tails of two and a half beads* at both ends. This striking and relevant feature is fully consistent with the picture of a single magnet interacting with a chain, see Fig. 1. Thereby, it was indeed shown that the interaction energy becomes *negative* when the chain has at least six beads ($N_c = 6$ in Fig. 1 corresponding to $N_{tot} = 2N + 1 = 7$ with $N = 3$), corresponding exactly to two tails of two and a half beads with respect to the touching single magnet. In the next section, we will look for the overall ground state at prescribed number of magnets N_{tot}, and especially locate the regime of two-chain assemblies.

4. Ground state structure of self-assembly

4.1. Energy minimization with genetic algorithm

In that numerical part of the work, the reduced potential energy of interaction $U^{tot}_{N_{tot}}$ has been minimized by evolving transient configurations on a triangular lattice using genetic algorithm. In order to increase the chance of finding the ground state, we typically employ many independent populations of about 1000 initial configurations consisting of individual particles positions. The particle occupation on the triangular lattice is mapped on an array of 0s and 1s, meaning a particle is present at a certain position on lattice or not, respectively. The evolution starts from a population of randomly generated individuals (i.e., configurations), and consists of an iterative process of creation of the new generations. In each generation, the potential energy of interaction U^{tot}_{N} is evaluated for every individual in the population. The prime difference to usual deterministic minimization procedures is that multiple individuals are evolved in each step in a stochastic manner: A number of the best configurations are selected from the current population and modified (recombined and possibly randomly mutated) to form a new generation. The algorithm terminates when a prescribed maximum number of generations has been produced and no more improvement of the best individual(s) is achieved.

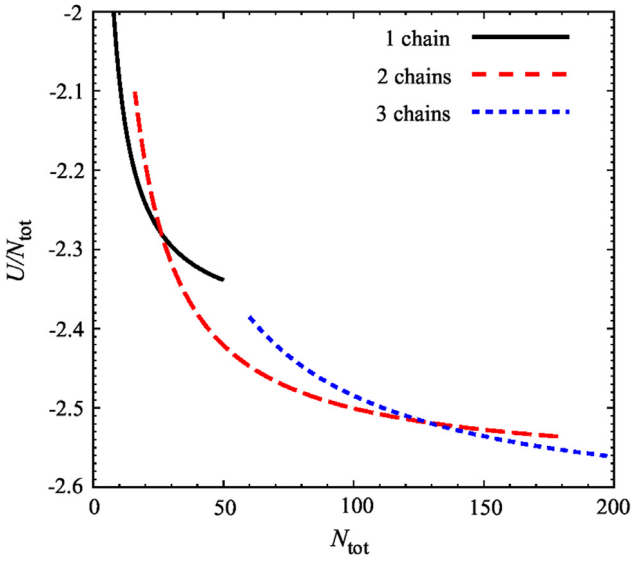

Fig. 7. Reduced energy per particle profiles as a function of the total number of particles N_{tot}. Ground states are as follows: one chain ($2 \leq N_{tot} \leq 26$), two chains ($27 \leq N_{tot} \leq 128$), and three chains from $N_{tot} \geq 129$.

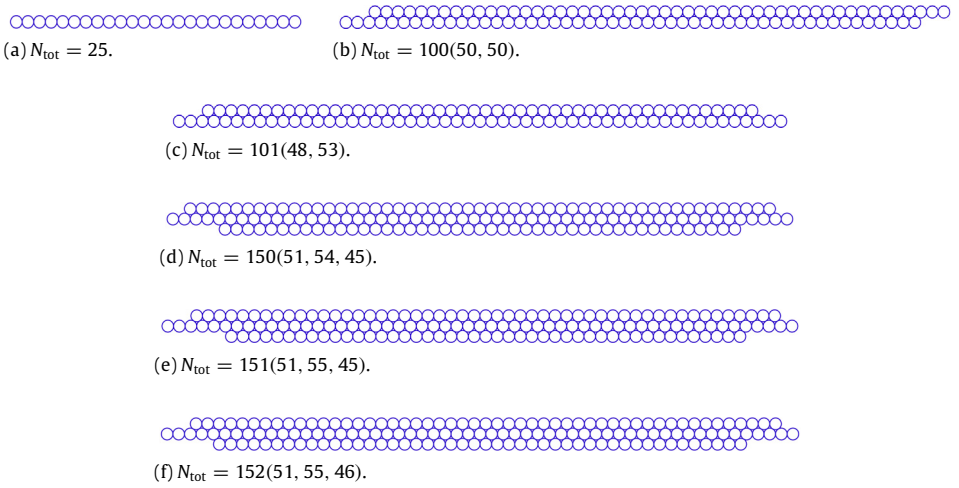

Fig. 8. Typical ground state microstructures for different total number of particles N_{tot}. (a) One-chain configuration for $N_{tot} = 25$. (b–f) Individual chain composition (from top to bottom) are indicated as (N_1, N_2), (N_1, N_2, N_3) (from left to right) for two- and three-chain configurations, respectively. (b, c) Two-chain configurations for $N_{tot} = 100, 101$, respectively. (d–f) Three-chain configurations for $N_{tot} = 150, 151, 152$, respectively.

4.2. Numerical results

The overall ground states at prescribed number of constitutive magnets N_{tot} were also independently computed using a genetic algorithm. The resulting energy profiles for one chain, two and three touching chains are depicted in Fig. 7. Corresponding illustrative microstructures are sketched in Fig. 8. The energy profile for the single chain structure stems from Eq. (6), whereas that for two touching chains was generated using Eqs. (9) and (13), for even and uneven number of particles respectively. In concordance with the magnetic energy analysis of two-chain states, see Figs. 3 and 5, minimization procedure based on genetic algorithm confirms, for $N_{tot} > 26$ (see Fig. 7), that the ground states correspond indeed to either

(i) two touching equally long parallel chains shifted by two and a half beads for even N_{tot}, see Fig. 8(b) for illustration,
(ii) or two symmetrically placed chains with $N + 3$ and $N - 2$ beads for uneven $N_{tot} = 2N + 1$, see Fig. 8(c) for illustration.

For $N_{tot} = 26$, the energy per bead for the one-chain structure is $u_{26}^{(1-chain)} \simeq -2.2791$ whereas for the two-chain structure $u_{26}^{(2-chains)} \simeq -2.2781$ is found. For $N_{tot} = 27$, we have $u_{27}^{(1-chain)} \simeq -2.2836$ against $u_{27}^{(2-chains)} \simeq -2.2889$.

Finally, we were able to locate the two- to three-chain transition at $N_{tot} = 129$ by means of genetic algorithm, cf. Fig. 7. More specifically, at $N_{tot} = 128$, the energy per bead for the two-chain structure is $u_{128}^{(2-chains)} \simeq -2.5182$ whereas

for the three-chain structure $u_{128}^{(3-chains)} \simeq -2.5178$ is found. At $N_{tot} = 129$, we have $u_{129}^{(2-chains)} \simeq -2.5187$ against $u_{129}^{(3-chains)} \simeq -2.5189$. Representative microstructures are depicted in Fig. 8(d–f), where it can be clearly identified that the (long) mid-chain is always sandwiched by two shorter chains. It is to say that the middle chain there plays a crucial role in stabilizing the two outer chains in registry.

5. Concluding remarks

We have analyzed the self-assembly of magnetic spheres under strong magnetic field in two dimensions. Chains and assembly of chains constitute the typical microstructures of magnetic beads. A simple but highly instructive situation concerns a single magnet (i.e., a monomer) interacting with a magnetic chain. An effective attraction, even with a dimer, sets in at very short separation as a result of *dipole–dipole correlations* and *excluded volume* effects. Nevertheless, a negative magnet–chain interaction energy is solely obtained for a long enough chain.

It turns out that the case of two-chain ground state structures possesses strong symmetry. This feature has allowed us to undertake exact analytical considerations about the behavior of the global potential of interaction. We have demonstrated that the attraction of parallel magnetic chains is essentially a near field effect (i.e., a range of the order of the magnetic monomer) and its strength strongly depends on chain length and relative position. In the far field limit, magnetic chains behave as super point-like dipoles as expected. Besides, we have brought to light tail creation as a mechanism for reduction (more negative) of the cohesive energy. A general result, which holds independently of number of particles, is that minimal energy is achieved if the tails have length of *two and a half* beads. In the case of even number of particles we obtain a two-fold symmetric ribbon made up of two shifted like-sized chains. For uneven number of particles, we obtain hat-like structures exhibiting a mirror symmetry.

Ground states of self-assembled magnets have been addressed by genetic algorithm. The resulting phase diagram (energy per bead vs the total number of beads N_{tot}) has the following characteristics: (i) At moderate number of beads $2 \leq N_{\text{tot}} \leq 26$, it is the *one-chain* assembly that possesses the lowest energy. (ii) When $27 \leq N_{\text{tot}} \leq 128$, it is the *two-chain* assembly that possesses the lowest energy. This is in excellent qualitative agreement with the experimental findings of Darras et al. [26] where they report the stability of two-chain ribbons above $N_{\text{tot}} = 30$. (iii) The *two-* to *three-chain* transition occurs at $N_{\text{tot}} = 129$. Again, the experimental findings of Darras et al. [26] agree well, where they report the stability of three-chain ribbons above $N_{\text{tot}} \approx 113$.

Note that analog findings to the three-chain structure were recently published [24] in three dimensions, where straight long magnetic chains develop a rodlike structure with a narrow rectangular section. Our work should shed some additional light on the mechanisms involved in the self-assembly observed recently in other experiments with magnetic colloidal particles exposed to a strong external field [8,25,28].

Acknowledgments

The authors acknowledge support from the bilateral Franco-Serbian PHC Pavle Savic 2014/15 Grant 32135NJ. I.S acknowledges financial support from Ministry of Education, Science, and Technological Development of the Republic of Serbia projects ON171017 and III45018, and European Commission under H2020 projects VI-SEEM and DAFNEOX (Grant No. 675121 and 645658). Numerical calculations were run on the PARADOX supercomputing facility at the Scientific Computing Laboratory of the Institute of Physics Belgrade.

References

[1] H. Zeng, J. Li, J.P. Liu, Z.L. Wang, S. Sun, Nature 420 (2002) 395.
[2] M. Wang, L. He, Y. Yin, Mater. Today 16 (2013) 110.
[3] A. Yethiraj, A. van Blaaderen, Nature 421 (2003) 513.
[4] V. Malik, A.V. Petukhov, L. He, Y. Yin, M. Schmidt, Langmuir 28 (2012) 14777.
[5] G. Pal, F. Kun, I. Varga, D. Sohler, G. Sun, Phys. Rev. E 83 (2011) 061504.
[6] R. Messina, L.A. Khalil, I. Stankovic, Phys. Rev. E 89 (2014) 011202(R).
[7] R. Messina, I. Stankovic, Europhys. Lett. 110 (2015) 46003.
[8] S. Mehdizadeh Taheri, et al., PNAS 112 (2015) 14484.
[9] R.M. Erb, et al., Nature 457 (2009) 999.
[10] E.D. Spoerke, G.D. Bachand, J. Liu, D. Sasaki, B.C. Bunker, Langmuir 24 (2008) 7039–7043.
[11] G. Singh, et al., Science 345 (2014) 1149.
[12] I. Stankovic, M. Dasic, R. Messina, Soft Matter (2016). http://dx.doi.org/10.1039/c5sm02774h.
[13] L. Kocbach, S. Lubbad, Phys. Educ. 45 (2010) 345.
[14] N. Vandewalle, S. Dorbolo, New J. Phys. 16 (2014) 013050.
[15] I.S. Jacobs, C.P. Bean, Phys. Rev. 100 (1955) 1060.
[16] P.G. de Gennes, P.A. Pincus, Phys. Kondens. Mater. 11 (1970) 189.
[17] T.A. Prokopieva, V.A. Danilov, S.S. Kantorovich, C. Holm, Phys. Rev. E 80 (2009) 031404.
[18] V. Danilov, T. Prokopyeva, S. Kantorovich, Phys. Rev. E 86 (2012) 061408.
[19] A. Kaiser, K. Popowa, H. Löwen, Phys. Rev. E 92 (2015) 012301.
[20] D. Heinrich, A.R. Goni, A. Smessaert, S.H.L. Klapp, L.M.C. Cerioni, T.M. Osan, D.J. Pusiol, C. Thomsen, Phys. Rev. Lett. 106 (2011) 208301.
[21] T.C. Halsey, W. Toor, Phys. Rev. Lett. 65 (1990) 2820;
T.C. Halsey, W. Toor, J. Stat. Phys. 61 (1990) 1257.

[22] R. Tao, J.M. Sun, Phys. Rev. Lett. 67 (1991) 398.
[23] T. Friedrich, I. Rehberg, R. Richter, Phys. Rev. E 91 (2015) 057201.
[24] R. Messina, I. Stankovic, Phys. Rev. E 91 (2015) 057202.
[25] S.G. Jones, et al., Soft Matter (2016). http://dx.doi.org/10.1039/c5sm03104d.
[26] Darras, et al., Eur. Phys. J. E 39 (2016) 47. http://dx.doi.org/10.1140/epje/i2016-16047-0.
[27] L.Yu. Iskakova, A.Yu Zubarev, Phys. Rev. E 66 (2002) 041405;
A.Yu. Zubarev, L.Yu. Iskakova, Phys. Rev. E 68 (2003) 061203;
L.Yu. Iskakova, G.A. Smelchakova, A.Yu. Zubarev, Phys. Rev. E 79 (2009) 011401.
[28] Klokkenburg, et al., Phys. Rev. Lett. 97 (2006) 185702.